Optimal Gaits for Mechanical Rectifier Systems

Justin Blair and Tetsuya Iwasaki, *Fellow, IEEE*

***Abstract*—The essential mechanism underlying animal locomotion can be viewed as mechanical rectification that converts periodic body movements to thrust force through interactions with the environment. This paper defines a general class of mechanical rectifiers as multi-body systems equipped with such thrust generation mechanisms. A simple model is developed from the Euler–Lagrange equation by assuming small body oscillations around a given nominal posture. The model reveals that the rectifying dynamics can be captured by a bilinear, but not linear, term of body shape variables. An optimal gait problem is formulated for the bilinear rectifier model as a minimization of a quadratic cost function over the set of periodic functions subject to a constraint on the average locomotion velocity. We prove that a globally optimal solution is given by a harmonic gait that can be found by generalized eigenvalue computation with a line search over cycle frequencies. We provide case studies of a chain of links for which snake-like undulations and jellyfish-like flapping gaits are found to be optimal.**

***Index Terms*—Biological control systems, locomotion, motion-planning, optimal control.**

I. Introduction

INSPIRATIONS from animal locomotion can provide a framework for designing robotic vehicles capable of robustly maintaining velocity by adaptively changing propulsion strategy as the surrounding environment changes. Animal locomotion may be viewed as a process of mechanical rectification [1], [2] in which a periodic body motion is converted to sustained thrust force through dynamic interactions with the environment. A specific motion pattern (or "gait") is chosen by each animal, depending upon the given environment, desired locomotion speed and range, disability conditions on the body, and other factors [3]–[6]. A fundamental problem in designing robotic locomotors, as well as in understanding animal locomotion mechanisms, is to determine a gait that optimizes a quantity representing the cost and/or performance, such as input energy.

Optimal gaits have been investigated in the literature on robotic locomotors. One approach is based on biological inspirations, wherein a particular gait, observed in animal locomotion, is parameterized and examined for optimality with respect to a cost function. Optimizations are typically performed via gridding of the parameter space and numerical simulations. This type of approach has been taken to search for optimal gaits for robots that mimic human walking [7], snake crawling [8], and anguilliform swimming [9]. Methods such as these might obtain an optimal parameter set within the particular gait examined, but may miss globally optimal gaits that differ from what is observed in biology.

Other approaches to find optimal gaits are based on some standard formulations of optimal control problems and various combinations of existing optimization methods. A popular method is to expand the signals over a finite set of basis functions, reducing the problem to a parametric optimization. Reference [10] used this method to find an optimal gait for eel swimming, where the necessary condition for optimality was solved using Newton iteration. This method is also used for biped walking with the aid of sequential quadratic programming [11], [12]. Another well known method is to apply the calculus of variations to reduce the optimization to a two-point boundary-value problem. This method has been used by [13] for nonholonomic locomotion systems, by [14] for a seven-link biped robot, and by [15] for shape actuated locomotion systems. While it would be ideal to have global solutions to general optimal control problems, most, if not all, of the currently available methods guarantee local optimality at best. This means that the solution depends on the initial condition of the numerical search in general, and thus can be far from the global optimum.

In this paper, we take a different approach, focusing on systems which are in continual contact with the environment (including swimming and slithering, but excluding walking). Instead of searching for locally optimal gaits for a fully nonlinear model of a locomotor system, we will first simplify the model through techniques such as Taylor series and describing function, and then develop a method for finding globally optimal gaits. In this way, potential suboptimality is not hidden behind the numerical optimization procedure, but is explicit in the problem formulation. The optimal gait for the simplified model could then be used as an initial condition in a local optimization for the original model. Thus, our method can be viewed as a complement to, rather than a replacement of, existing local optimization methods. The process to compute our solution is extremely fast and numerically stable. Hence, it can be applied to hyper-redundant rectifier systems with many degrees of freedom. Another advantage is that an optimal gait is found within those achievable by the given set of actuators. This feature is especially important for underactuated systems that have less actuators than the number of shape variables because not all gaits are achievable by a small number of actuators.

Manuscript received April 25, 2009; revised January 14, 2010, and March 23, 2010; accepted March 23, 2010. Date of publication May 24, 2010; date of current version January 12, 2011. This work is supported by the National Science Foundation under 0237708 and 0654070, and by the Office of Naval Research, under MURI Grant N00014-08-1-0642. Recommended by Associate Editor P. Tsiotras.

J. Blair is with Department of Mechanical and Aerospace Engineering, University of Virginia, Charlottesville, VA 22904 USA (e-mail: jtb8s@virginia.edu).

T. Iwasaki is with the Department of Mechanical and Aerospace Engineering, University of California, Los Angeles, CA 90095 USA (e-mail: tiwasaki@ucla.edu).

Color versions of one or more of the figures in this paper are available online at http://ieeexplore.ieee.org.

Digital Object Identifier 10.1109/TAC.2010.2051074

To this end, we first define a general class of mechanical rectifiers which capture the essential dynamics of animal locomotion, develop equations of motion, and then approximate the system by assuming small perturbations around a nominal posture. It turns out that a linear approximation fails to capture the rectifying dynamics; the simplest model should contain a bilinear term of the shape variables and their derivatives. An optimal gait problem is then formulated for the bilinear rectifier model, where a quadratic cost function is minimized over the set of periodic body movements achievable by control inputs, subject to an equality constraint on the average locomotion velocity. The problem belongs to the class of infinite dimensional nonconvex problems that are extremely difficult in general. However, our result reveals that a globally optimal gait is purely sinusoidal and can be found by calculating the generalized eigenvalues of a pair of Hermitian matrices and by sweeping over the frequency.

Several case studies are provided. We consider a mechanical rectifier formed as a chain of multiple links subject to environmental forces with directional preference. It is demonstrated that natural gaits similar to those observed in animal locomotion can be found, without any *a priori* assumptions, through minimization of such cost functions as input power, rate of shape change, and torque derivative. In particular, undulatory gaits similar to snake crawling or leech/lamprey swimming are found to be optimal if the nominal posture is straight, while flapping gaits observed in jellyfish-like animals are optimal if the nominal posture is curved. We also consider a disk-mass system that captures the rectifying dynamics in the simplest manner. Analytical expressions of optimal gaits are obtained for this simple case, and are used to make some general observations through analogy to more complex rectifiers, suggesting how system parameters affect the gait.

Conference versions of this paper have appeared in [16] and [17], where optimal gaits were sought over the set of harmonic signals and solutions were given without details of proofs. This paper extends the previous results to the case of general periodic signals and provides complete proofs. Derivations of the general rectifier equations are also new in the present paper.

Notation: The sets of n by m real and complex matrices are denoted by $\mathbb{R}^{n\times m}$ and $\mathbb{C}^{n\times m}$, respectively, where the dimensional notation is omitted if $m=1$ or $n=m=1$. The set of positive real numbers is $\mathbb{R}_+$. The set of positive integers is denoted by $\mathbb{Z}$, and its subset up to k by $\mathbb{Z}_k$. Let $\mathbb{Z}_\infty := \mathbb{Z}\cup\{\infty\}$. For matrices M_i with $i\in\mathbb{Z}_k$, the matrix obtained by stacking them in a column is denoted by $\mathrm{col}(M_1,\dots,M_k)$, and we use $\mathrm{diag}(M_1,\dots,M_k)$ if they are stacked on the diagonal. When the argument is a single vector v, $\mathrm{diag}(v)$ is the diagonal matrix whose i^{th} diagonal entry is v_i. For a complex matrix M, its transpose, complex conjugate transpose, and real part are denoted by M^{T}, M^*, and $\Re[M]$, respectively. For a generic function $F(x)$ and $h\in\mathbb{Z}_\infty$, define

$$F^h(x) := \mathrm{diag}\left(F(x), F(2x), \dots, F(hx)\right).$$

If F is a constant matrix, F^h is the block diagonal matrix having F repeated h times on the diagonal. For a differentiable mapping $f:\mathbb{R}^n\to\mathbb{R}^m$ of variable $x\in\mathbb{R}^n$, its partial derivative $\partial f/\partial x$ is the $n\times m$ matrix with (i,j) entry $\partial f_j/\partial x_i$.

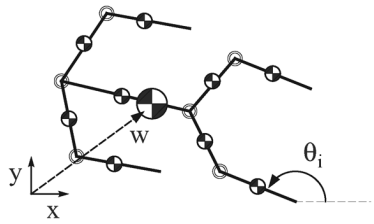

Fig. 1. Multilink swimming system.

The set of all T-periodic, unbiased, continuously differentiable, possibly vector-valued functions is denoted by $\mathbb{P}_T$. For $h\in\mathbb{Z}$, the finite dimensional subspace of $\mathbb{P}_T$ spanned by harmonics up to the h^{th} order is denoted by $\mathbb{P}_T^h$. For consistency, we also define $\mathbb{P}_T^\infty := \mathbb{P}_T$. The phasor $\hat{x}$ of $x\in\mathbb{P}_T^h$ with $h\in\mathbb{Z}_\infty$ is defined by the coefficients of the complex Fourier series as follows:

$$x(t) = \sum_{k=1}^{h} \Re[\hat{x}_k e^{jk\omega t}], \quad \hat{x} := \mathrm{col}(\hat{x}_1, \hat{x}_2, \dots, \hat{x}_h)$$

where $\omega := 2\pi/T$, and $\hat{x}_k$ is called the k^{th} phasor of x. Let $\mathbf{\Pi}$ be the set of transfer functions $\Pi(s)$ of the form $\Pi(s) = F(-s)^{\mathsf{T}}\Psi F(s)$, where Ψ is a constant Hermitian matrix and $F(s)$ is a linear combination of stable (proper) transfer functions and differentiators. If an input $\mu\in\mathbb{P}_T$ is applied to $F(s)$, the output is given by $y+\tilde{y}$ where y is the steady state response that is T-periodic, and $\tilde{y}$ is the transient response that eventually dies out. With a slight abuse of notation, we denote the T-periodic signal $y^{\mathsf{T}}\Psi y$ by $\mu^{\mathsf{T}}\overset{\circ}{\Pi}\mu$. This notation is motivated by the fact (see Lemma 4 in Appendix A) that the average value of $y^{\mathsf{T}}\Psi y$ over a cycle is given by $\hat{\mu}^*\Pi(j\omega)\hat{\mu}/2$ when μ is sinusoidal (i.e., $\mu\in\mathbb{P}_T^1$).

II. Mechanical Rectifier Systems

Consider a multi-body mechanical system placed in an environment of up to three spatial dimensions. The bodies are rigid, and are connected to each other through rigid or flexible mechanisms (e.g., rotational joints as in manipulator arms [18] and flexible wires as in tensegrity structures [19], [20]). The system is equipped with actuators, each a local input force that acts between bodies and producing no global thrust with respect to the environment. For example, motors may drive joints and linear actuators may push and pull links relative to one another, but there are no jet engines. The motion of the bodies produce interactive forces and torques from the environment, and when periodic motion can result in a net thrust due to those interactive forces, we call the system a *mechanical rectifier* [21], [22].

We restrict our attention to systems that *continually* interact with the environment. This excludes systems such as walking robots but still includes a wide range of other animal locomotions, such as swimming, crawling (as in snakes), and flying. The multilink robot inspired by swimming frogs, depicted in Fig. 1, is one such example.

The following sections first develop equations of motion for a general class of mechanical rectifiers in up to three spatial dimensions, then derive an approximate quadratic system that captures and reveals the mechanism of rectification.

A. General Equations of Motion

To derive the equations of motion for a general multibody rectifier system, we begin with the well known Euler-Lagrange equation:

$$\frac{d}{dt}\left(\frac{\partial L}{\partial \dot{q}}\right) - \frac{\partial L}{\partial q} = \psi \tag{1}$$

where $q(t) \in \mathbb{R}^n$ are the generalized coordinates, $\psi(t) \in \mathbb{R}^n$ are the generalized forces, and $L(q,\dot{q}) := T - V \in \mathbb{R}$ is the difference between the kinetic energy $T(q,\dot{q})$ and the potential energy $V(q)$. The generalized force ψ is defined by

$$\delta W = (\delta q)^{\mathsf{T}} \psi \tag{2}$$

where δW is the virtual work done by external forces and torques, and δq is the virtual displacement in generalized coordinates. Let us split the generalized coordinates q into two parts

$$q = \begin{bmatrix} \theta \\ w \end{bmatrix}$$

where $w(t) \in \mathbb{R}^p$ is the global position vector for the center of mass of the system relative to the environment (the spatial dimension is $p = 1$, 2, or 3), and $\theta(t) \in \mathbb{R}^n$ contains the variables specifying the local shape and global orientation of the bodies. It is assumed that the kinetic energy T and potential energy V are given by

$$T = \frac{1}{2}\left(\dot{\theta}^{\mathsf{T}} J(\theta)\dot{\theta} + m\dot{w}^{\mathsf{T}}\dot{w}\right), \quad V = E(\theta) + mg^{\mathsf{T}} w$$

where $J(\theta)$ is the inertia matrix, m is the total mass of the system, $E(\theta)$ is the elastic energy stored in the system, and g is the net gravity (buoyancy) vector. We consider the case where the generalized force consists of environmental forces, actuator inputs, and dissipative effects such as joint frictions.

Assembling all the generalized forces (details will be given in the next section) and exploiting the structures of the kinetic and potential energies, the equations of motion for general rectifier systems are given by the following form:

$$\begin{aligned} &J(\theta)\ddot{\theta} + C(\theta,\dot{\theta})\dot{\theta} + k(\theta) + d(\theta,\dot{\theta}) \\ &\quad + R(\theta)^{\mathsf{T}}\gamma(R(\theta)\dot{\theta} + N(\theta)\dot{w}) = B(\theta)u, \\ &m\ddot{w} + mg + N(\theta)^{\mathsf{T}}\gamma\left(R(\theta)\dot{\theta} + N(\theta)\dot{w}\right) = 0 \end{aligned} \tag{3}$$

where the terms $J(\theta)\ddot{\theta} + C(\theta,\dot{\theta})\dot{\theta}$ and $m\ddot{w}$ are the inertial torques and forces, $k(\theta) + d(\theta,\dot{\theta})$ are the torques due to body stiffness and damping, $u(t) \in \mathbb{R}^\ell$ is the applied input, the terms involving γ capture the effect of environmental forces, and

$$C(\theta,\dot{\theta}) := \left(\frac{\partial J(\theta)\dot{\theta}}{\partial \theta}\right)^{\mathsf{T}} - \frac{1}{2}\left(\frac{\partial J(\theta)\dot{\theta}}{\partial \theta}\right), \quad k(\theta) := \frac{\partial E(\theta)}{\partial \theta}.$$

The quantity $R(\theta)\dot{\theta} + N(\theta)\dot{w}$ is the vector of link velocities in the body coordinates, relative to the environment. The function $\gamma : \mathbb{R}^\sigma \to \mathbb{R}^\sigma$ is a possibly nonlinear mapping that generates the forces and torques resulting from the relative motion. Typically, γ satisfies the sector condition $y_i x_i \geq 0$ for each entry of the input/output pair $y = \gamma(x)$. We see from (3) that the applied input u changes the shape and orientation θ, which in turn drives the global position w through interactions with the environment. In particular, a periodic motion θ, generated by a periodic input u via the first equation, can be rectified through the second equation to result in a "locomotion" with velocity $\dot{w}$.

B. Derivation of the Generalized Force

We now provide a detailed derivation of the generalized force ψ that leads to terms in (3). Specifically, we will derive the three terms in $\psi = \psi_e + \psi_a + \psi_d$ where ψ_e is the environmental force, ψ_a is the actuator force, and ψ_d is the dissipative force, respectively. In the development, "forces" are meant to include both linear forces and rotational torques, and similar generalizations apply to "displacements," "velocities," and "coordinates."

1) Environmental Forces: We assume that the effect of the environmental forces on the system can be approximately represented by forces acting on a finite number of points on the bodies. Let r be a vector indicating the Cartesian coordinates of such points, and f be the corresponding vector of forces acting on them. The velocity of the points relative to the environment, $\dot{r}$, can be expressed as $\Omega(\theta)\dot{r}$ in the body coordinates, where $\Omega(\theta)$ is the rotation matrix that transforms a vector from the inertial frame to the body frame. Assume that the environmental force is a (possibly nonlinear) function of the relative velocity and is given by $-\gamma(\Omega(\theta)\dot{r})$ in the body frame. Transforming it back to the inertial frame, the environmental force is given by

$$f = -\Omega(\theta)^{\mathsf{T}}\gamma\left(\Omega(\theta)\dot{r}\right). \tag{4}$$

Note that the Cartesian coordinates r are linear in w. In fact, it would have the form $r(q) = \rho(w) + \epsilon(\theta)$ for some functions ρ and ϵ where the former is linear. We then have

$$\dot{r} = \left(\frac{\partial r}{\partial \theta}\right)^{\mathsf{T}}\dot{\theta} + \left(\frac{\partial r}{\partial w}\right)^{\mathsf{T}}\dot{w}$$

where the coefficient of $\dot{w}$ is constant. The virtual work done by the environmental force is $\delta W_e = (\delta r)^{\mathsf{T}} f = (\delta q)^{\mathsf{T}}\psi_e$, from which we obtain the corresponding generalized force

$$\psi_e = \frac{\partial r}{\partial q} f = -\begin{bmatrix} R(\theta)^{\mathsf{T}} \\ N(\theta)^{\mathsf{T}} \end{bmatrix}\gamma\left(R(\theta)\dot{\theta} + N(\theta)\dot{w}\right)$$

where

$$R(\theta) := \Omega(\theta)\left(\frac{\partial r}{\partial \theta}\right)^{\mathsf{T}}, \quad N(\theta) := \Omega(\theta)\left(\frac{\partial r}{\partial w}\right)^{\mathsf{T}}.$$

2) Actuator Forces: Let ϕ_i be the displacement of the i^{th} actuator (e.g., the joint angle driven by a rotary motor or displacement of a linear motor) and let u_i be the force or torque generated. Define $\phi \in \mathbb{R}^\ell$ and $u \in \mathbb{R}^\ell$ by stacking ϕ_i and u_i in columns where ℓ is the number of actuators. Suppose that ϕ is a differentiable function of θ and is independent of w due to the assumption that all actuators are local (only generating forces/torques between bodies). The virtual work done by the actuators is

$$\delta W_a = (\delta\phi)^{\mathsf{T}} u = (\delta\theta)^{\mathsf{T}}\frac{\partial \phi}{\partial \theta} u.$$

Hence, from (2), the generalized forces due to the actuators are given by

$$\psi_a = \begin{bmatrix} B(\theta)u \\ 0 \end{bmatrix}, \quad B(\theta) := \frac{\partial \phi}{\partial \theta}.$$

Note that $B(\theta)$ is a constant matrix if ϕ is a linear function of θ, which is the case when, e.g., θ contains all the joint angles and ϕ consists of those actuated. The matrix $B(\theta)$ depends on θ in general, as is the case if a body is driven by a linear actuator attached to another body, similar to skeletal muscles.

3) Dissipative Forces: Let φ be the vector of relative displacements of two bodies between which dissipative forces like frictions exist. The variable φ is a function of θ, but not w, since the dissipation effect due to the interactions with the environment is captured within the environmental force. Let us assume that the dissipative forces experienced through displacement φ is a differentiable function of $\dot{\varphi}$, denoted by $-\mu(\dot{\varphi})$. Typically, the function μ is a diagonal mapping such that each diagonal entry satisfies the sector condition $\mu_i(\dot{\varphi}_i)\dot{\varphi}_i > 0$. The virtual work done by the dissipative forces is

$$\delta W_d = -(\delta\varphi)^{\mathsf{T}}\mu(\dot{\varphi}) = -(\delta\theta)^{\mathsf{T}}\frac{\partial \varphi}{\partial \theta}\mu\left(\left(\frac{\partial \varphi}{\partial \theta}\right)^{\mathsf{T}}\dot{\theta}\right)$$

from which we obtain the associated generalized forces

$$\phi_d = \begin{bmatrix} -d(\theta,\dot{\theta}) \\ 0 \end{bmatrix}, \quad d(\theta,\dot{\theta}) := \frac{\partial \varphi}{\partial \theta}\mu\left(\left(\frac{\partial \varphi}{\partial \theta}\right)^{\mathsf{T}}\dot{\theta}\right).$$

If μ represents linear (viscous) damping, then the generalized forces have the form $d(\theta,\dot{\theta}) = D(\theta)\dot{\theta}$ for some positive (semi)definite matrix $D(\theta)$. If φ is a linear function of θ (e.g., joint angles), then $d(\theta,\dot{\theta})$ becomes independent of θ.

III. Mechanisms Underlying Thrust Generation

To gain insight into the locomotion mechanism of rectifier systems, we attempt to analyze the behavior of the rectifier (3) through the simplest approximate model that captures the essential dynamics of rectification. This section develops such a simple model and reveals the mechanism underlying rectification of periodic body motion θ to yield global velocity $\dot{w}$. In the rest of this paper, we consider for simplicity the case where the effect of the gravity potential can be neglected (swimming of a neutrally buoyant system, crawling on the horizontal plane, etc.), and set $g = 0$ in (3).

A. Nominal Posture and Approximation

Many biological systems are observed to take a particular posture for relaxed cruising between active locomotion phases. For instance, a fish cruises with a straight body posture, while a ray cruises with a posture resembling a fixed-wing aircraft. Motivated by these cruising postures, we introduce the notion of a *nominal posture*. A posture of the rectifier specified by the shape and orientation $\theta(t) = \eta \in \mathbb{R}^n$ is said to be nominal at velocity $\dot{w}(t) = v_o \in \mathbb{R}^p$ if

$$\begin{aligned} &R(\eta)^{\mathsf{T}}\gamma\left(N(\eta)v_o\right) + k(\eta) = 0, \\ &\delta := N(\eta)^{\mathsf{T}}\gamma\left(N(\eta)v_o\right) \in \mathbb{V} \end{aligned} \tag{5}$$

where $\mathbb{V}$ is the straight line in $\mathbb{R}^p$ that is parallel to v_o and passes through the origin, indicating the direction of locomotion. Condition (5) means that if the rectifier takes a nominal posture η at velocity v_o and receives a (fictitious) external force in the direction of v_o to balance out the environmental drag δ, then the locomotion velocity and body shape/orientation are simultaneously maintained, i.e., $\dot{w}(t) \equiv v_o$ and $\theta(t) \equiv \eta$, in the absence of any actuating input u. Certain periodic body motion θ about a nominal posture η, generated by actuator input u, is expected to produce the necessary thrust for the system that balances out the drag and maintains locomotion at the average velocity v_o. Throughout the paper, we choose the global coordinate frame so that its first axis is aligned with $\mathbb{V}$, that is, $v_o = \nu e_1$ for some $\nu \in \mathbb{R}$ where $e_i \in \mathbb{R}^p$ is the vector whose i^{th} entry is one and the others are zero.

We now consider a periodic body motion $\theta(t)$ about a nominal posture η at velocity v_o, and assume that small oscillation of $\vartheta(t) := \theta(t) - \eta$ maintains the locomotion velocity $\dot{w}(t)$ near v_o. To simplify the equations of motion in (3), we first linearize the environmental force function γ using the Taylor series (slope at a nominal operating point) or the describing function (average slope in the operating region) [23]. While such approximation could introduce a potentially large error in general, qualitative characteristics of the environmental forces, that are important for shaping the gait, may be captured. For instance, anisotropy of normal and tangential forces, which is known to be essential for undulatory locomotion [8], [24], [25], can be well captured by linear models [8]. For further simplification, the nonlinear equations of motion in (3) may be linearized by expanding each expression into its Taylor series in terms of ϑ, and keeping up to the first order terms. However, as shown shortly, the essential dynamics for rectification turns out to be embedded in the second or higher order terms in the second equation of (3), and hence the linearized model fails to capture the locomotion dynamics. For this reason, we choose to linearize the first equation in terms of ϑ but keep up to the second order terms in the second equation. In particular, we make the following approximations:

$$\begin{aligned} &\begin{bmatrix} R(\theta)^{\mathsf{T}} \\ N(\theta)^{\mathsf{T}} \end{bmatrix}\gamma\left(R(\theta)\dot{\theta} + N(\theta)\dot{w}\right) \cong \begin{bmatrix} D_1 & A(\vartheta) \\ A(\vartheta)^{\mathsf{T}} & Q(\vartheta) \end{bmatrix}\begin{bmatrix} \dot{\vartheta} \\ \dot{w} \end{bmatrix}, \\ &J(\theta) \cong J(\eta) =: J, \quad B(\theta) \cong B(\eta) =: B, \\ &k(\theta) \cong k(\eta) + K\vartheta, \quad d(\theta,\dot{\theta}) \cong D_2\dot{\vartheta} \end{aligned}$$

where J, D_1, D_2, K, and B are constant matrices,[1] $A(\vartheta)$ is affine in ϑ, and $Q(\vartheta)$ is quadratic in ϑ. Hence, assuming that $\vartheta(t)$ and its derivatives are small, and that $\dot{w}(t) \cong v_o$, the general equations of motion in (3) are approximated by

$$\begin{aligned} J\ddot{\vartheta} + D\dot{\vartheta} + K\vartheta + L(\vartheta)v &= Bu, \\ m\dot{v} + A(\vartheta)^{\mathsf{T}}\dot{\vartheta} + Q(\vartheta)v &= 0 \end{aligned} \tag{6}$$

where $D := D_1 + D_2$, $L(\vartheta) := A(\vartheta) - A(0)$, and $v(t) := \dot{w}(t)$ is the velocity of the center of mass. We shall call the system (6) a *bilinear rectifier* since the essential mechanism for thrust generation is captured by the bilinear term $A(\vartheta)^{\mathsf{T}}\dot{\vartheta}$ as explained in the next section.

[1]With a slight abuse of notation, we use symbol J to denote the nominal value of $J(\theta)$, and similarly for B.

B. Bilinear Mechanism for Rectification

The dynamics of rectification are transparent in the simplified equations of motion (6). In particular, the second equation shows that a periodic body movement $\vartheta(t)$ leads to the thrust $-A(\vartheta)^{\mathsf{T}}\dot{\vartheta}$ and drag $Q(\vartheta)v$. The difference between the two gives the acceleration term $m\dot{v}$, and the thrust and drag should balance on average during the steady state locomotion. A close look at the thrust term reveals that the essential dynamics of rectification are captured by the skew-symmetric part of the linear coefficient matrix in $A(\vartheta)$. To explain this, let us consider the simple case where the direction of locomotion is fixed ($p = 1$) and define $\Lambda \in \mathbb{R}^{n\times n}$ by $A(\vartheta) = \Lambda\vartheta + A(0)$. Then the average thrust α over a cycle of periodic motion is given by

$$\alpha = -\int_0^T A(\vartheta)^{\mathsf{T}}\dot{\vartheta}dt = -\int_0^T \dot{\vartheta}^{\mathsf{T}} S\vartheta dt, \quad S := \frac{\Lambda - \Lambda^{\mathsf{T}}}{2} \tag{7}$$

where T is the period of $\vartheta(t)$, and we noted that the integral of $\dot{\vartheta}P\vartheta$ over a cycle is zero for any periodic signal ϑ and for an arbitrary symmetric matrix P. We now see that the periodic motion $\vartheta(t)$ is rectified through the bilinear mechanism $\dot{\vartheta}^{\mathsf{T}}S\vartheta$ in (7) to generate the thrust. This observation motivates us to call (6) the bilinear rectifier. It should be emphasized that, if the original equations of motion (3) are linearized in terms of ϑ, then we have $\Lambda = 0$ and the resulting approximation fails to capture the thrust essential for locomotion.

The bilinear mechanism in (7) is a generalization of the rectifying dynamics studied by Brockett [2], [26], where $\dot{\vartheta}^{\mathsf{T}}S\vartheta$ takes the form $\vartheta_1\dot{\vartheta}_2 - \vartheta_2\dot{\vartheta}_1$, representing a canonical dynamics for rectification. The basic mechanism for gait selection is embedded in the eigenvectors of S. We have shown [22] that the eigenvector ϑ_o of jS associated with the maximum eigenvalue λ_o gives the basic gait, which maximizes the thrust to velocity ratio at a given cycle frequency ω

$$\max_{\vartheta\in\mathbb{P}_T} \frac{\int_0^T(-\dot{\vartheta}^{\mathsf{T}}S\vartheta)dt}{\int_0^T \|\cdot\vartheta\|^2 dt} = \max_{\hat{\vartheta}\in\mathbb{C}^n} \frac{j\hat{\vartheta}^* S\hat{\vartheta}}{\omega\|\hat{\vartheta}\|^2} = \frac{\lambda_o}{\omega} \tag{8}$$

where $T := 2\pi/\omega$ and the maximum is attained at $\hat{\vartheta} = \vartheta_o$ or $\vartheta(t) = \Re[\vartheta_o e^{j\omega t}]$. The resulting gait $\vartheta(t)$ turns out to be a circle on the $(\vartheta_1, \vartheta_2)$ plane for Brockett's canonical rectifier, and a body undulation with traveling waves for a robotic snake [8]. Optimality criteria for gait selection would also include other factors such as energy consumption and amplitudes of control inputs and motion variables. The optimal gaits with respect to such criteria turn out to be variations of the basic gait embedded in the bilinear rectification mechanism.

IV. Optimal Locomotion of the Bilinear Rectifier

In this section, we first formulate an optimal locomotion problem to find a gait (periodic ϑ) that minimizes a quadratic cost function for the mechanical rectifier. The problem is difficult, so we reformulate it for tractability using the standard averaging technique, and finally give a globally optimal solution to the modified problem. The optimal gait theory will be developed for the bilinear rectifier (6), but the result will be validated later for the original fully nonlinear system (3) through numerical simulations.

TABLE I
Objective Functions Specified by Π

Quantity	Objective Integral	$\Pi(j\omega)$
Perturbation from η	$\frac{1}{T}\int_0^T \|\vartheta\|^2 dt$	$\begin{bmatrix} I & 0 \\ 0 & 0 \end{bmatrix}$
Shape Magnitude	$\frac{1}{T}\int_0^T \|\varphi\|^2 dt$	$\begin{bmatrix} W^{\mathsf{T}}W & 0 \\ 0 & 0 \end{bmatrix}$
Shape Derivative	$\frac{1}{T}\int_0^T \|\dot{\varphi}\|^2 dt$	$\begin{bmatrix} \omega^2 W^{\mathsf{T}}W & 0 \\ 0 & 0 \end{bmatrix}$
Input Torque	$\frac{1}{T}\int_0^T \|u\|^2 dt$	$\begin{bmatrix} 0 & 0 \\ 0 & I \end{bmatrix}$
Input Torque Rate	$\frac{1}{T}\int_0^T \|\dot{u}\|^2 dt$	$\begin{bmatrix} 0 & 0 \\ 0 & \omega^2 I \end{bmatrix}$
Input Power	$\frac{1}{T}\int_0^T \dot{\theta}^{\mathsf{T}} B u dt$	$\frac{1}{2}\begin{bmatrix} 0 & -j\omega B \\ j\omega B^{\mathsf{T}} & 0 \end{bmatrix}$

A. Problem Formulation

Consider the mechanical rectifier (6) with nominal posture η at locomotion velocity v_o. We would like to find an optimal gait $\vartheta(t)$ (and the control input $u(t)$ achieving the gait) that minimizes a quadratic cost function subject to the constraint that the average velocity of locomotion is v_o. The problem can be formulated as the following optimization over the set of T-periodic signals $\mathbb{P}_T$:

$$\min_{\substack{T\in\mathbb{R}_+ \\ v,\vartheta,u\in\mathbb{P}_T}} \frac{1}{T}\int_0^T \begin{bmatrix}\vartheta \\ u\end{bmatrix}^{\mathsf{T}} \overset{\circ}{\Pi} \begin{bmatrix}\vartheta \\ u\end{bmatrix} dt$$
$$\text{subject to} \quad \frac{1}{T}\int_0^T v dt = v_o \tag{9}$$

where u, ϑ, and v are signals satisfying (6), and $\Pi(s) \in \mathbb{\Pi}$ is a given transfer function. Without loss of generality, we assume that the locomotion is along the x-axis with speed $\nu \in \mathbb{R}$, so that $v_o = \nu e_1$.

The objective function is quadratic in ϑ and u, and through the choice of $\Pi(s)$, derivatives of ϑ and u may also be captured, representing many physical quantities. Table I provides a short list of such quantities and their associated weighting function $\Pi(j\omega)$, where $\varphi := W\vartheta$ is the vector of shape variables (e.g. joint angles) specified by a constant matrix W. The average value over one period is taken for input power, and mean-square values for the other quantities. The cost function can be made to include multiple objectives by taking a weighted sum of these (and other) quantities.

For the quadratic cost function with an arbitrary weighting Π_o, the solution to problem (9) may generate a gait with a large amplitude oscillation of ϑ, violating the small amplitude assumption imposed to derive the quadratic equations of motion in (6). Such gait may not be appropriate for the original equations of motion (3). To remedy this situation, one can penalize the amplitude of ϑ by setting

$$\Pi = (1-\beta)\Pi_{\mathrm{a}} + \beta\Pi_o \tag{10}$$

where Π_{a} corresponds to the first entry in Table I, and β is a weighting parameter satisfying $0 \le \beta \le 1$. When Π_{a} and Π_o define competing objectives, the amplitude of optimal ϑ would

be a nondecreasing function of β. The largest value of β can thus be found so as to satisfy a hard constraint on the amplitude of ϑ, if desired. This type of Pareto-optimal approach has been used for multiobjective H_2 control with a proof of convergence [27].

B. Tractable Reformulation

Let us now reformulate the problem in (9) for tractability by simplifying the constraints through the averaging technique. If $v(t) \cong v_o = \nu e_1$, it follows from averaging the second equation in (6) over a cycle that

$$\int_0^T \left((a_i + \vartheta^\mathsf{T} Q_i \vartheta)\nu + \dot{\vartheta}^\mathsf{T} \Lambda_i \vartheta dt \right) = 0 \tag{11}$$

holds approximately for $i \in \mathbb{Z}_p$, where a_i, Q_i, and Λ_i are the constants specified by

$$L(\vartheta)e_i = \Lambda_i \vartheta, \quad e_i^\mathsf{T} Q(\vartheta) e_1 = a_i + b_i^\mathsf{T}\vartheta + \vartheta^\mathsf{T} Q_i \vartheta.$$

Conversely, if (11) holds, then $v(t) \equiv v_o$ satisfies the second equation in (6) on average. Therefore, it appears reasonable to replace the velocity constraint in (9) and the second equation in (6) by the p equations in (11). Finally, let us define the following problem:

$$\begin{aligned} &\min_{\substack{T\in\mathbb{R}_+ \\ \vartheta,u\in\mathbb{P}_T}} \frac{1}{T}\int_0^T \begin{bmatrix}\vartheta \\ u\end{bmatrix}^\mathsf{T} \overset{\circ}{\Pi} \begin{bmatrix}\vartheta \\ u\end{bmatrix} dt \quad \text{subject to} \\ &\begin{cases} \int_0^T \left((a_1 + \vartheta^\mathsf{T} Q_1 \vartheta)\nu + \dot{\vartheta}^\mathsf{T}\Lambda_1\vartheta \right) dt = 0, \\ J\ddot{\vartheta} + D\dot{\vartheta} + (K + \nu\Lambda_1)\vartheta = Bu \end{cases} \end{aligned} \tag{12}$$

where the constraint (11) is imposed only for $i = 1$. We expect that a solution to this problem will automatically satisfy the remaining omitted acceleration constraints, i.e., (11) for $i = 2, \ldots, p$, on the grounds that acceleration in a direction normal to $\mathbb{V}$ would require a larger value of the objective function and would hence be eliminated. This is also what we have observed in all of our numerical studies.

The omission of constraints (11) for $i = 2, \ldots, p$ can be rigorously justified for certain practical cases. Recall that most animals have a body symmetric about an axis (or a plane), and the direction of locomotion is often chosen to be aligned with the axis of symmetry. A robotic locomotor may be designed to have this property. In this case, feasible gaits may be restricted to be symmetric about the $\mathbb{V}$ line, at the expense of potential increase in the cost function value. A benefit is that the symmetry can be exploited to make the gait optimization simpler. A symmetric gait would automatically lead to locomotion along the $\mathbb{V}$ line due to the balance of forces. The equations of motion (6) can then be given in terms of a reduced number of independent variables with only one degree of freedom in v, i.e., $p = 1$. For an example, the locomotor in Fig. 1 could be reduced to the system shown in Fig. 2, assuming that the arm and leg movements are symmetric about the dashed line. The reduction in the size of the optimization problem (the dimensions of ϑ and u) would generally lead to more efficient and reliable computation.

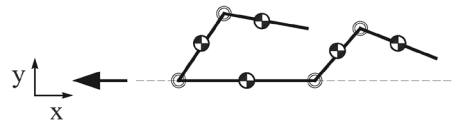

Fig. 2. Exploiting symmetry of the frog-like multilink system.

C. Globally Optimal Solution

This section presents an exact solution to the problem in (12). We first consider a finite dimensional approximation of the problem where the underlying space of periodic signals $\mathbb{P}_T$ in (12) is replaced by the subspace $\mathbb{P}_T^h$ spanned by the first h harmonics of the Fourier series expansion for a given $h \in \mathbb{Z}$. The following lemma reduces this modified problem to a constrained quadratic optimization.

Lemma 1: Let $h \in \mathbb{Z}$ be given, and consider the problem obtained by replacing $\mathbb{P}_T$ by $\mathbb{P}_T^h$ in (12). Define

$$\begin{aligned} X(\omega) &:= \frac{1}{2}\begin{bmatrix}P(\omega) \\ I\end{bmatrix}^* \Pi(j\omega) \begin{bmatrix}P(\omega) \\ I\end{bmatrix}, \\ Y(\omega) &:= P(\omega)^* \left(S(\omega) - \nu Q_1\right) P(\omega)/(2a_1\nu), \\ S(\omega) &:= j\omega\left(\Lambda_1 - \Lambda_1^\mathsf{T}\right)/2, \\ P(\omega) &:= (\nu\Lambda_1 + K + j\omega D - \omega^2 J)^{-1} B. \end{aligned} \tag{13}$$

Then the problem is equivalent to

$$\min_{\omega\in\mathbb{R}, \hat{u}\in\mathbb{C}^{\ell h}} \left\{ \hat{u}^* X^h(\omega)\hat{u} : \hat{u}^* Y^h(\omega)\hat{u} = 1 \right\}. \tag{14}$$

In particular, a solution $(\omega, \hat{u})$ to (14) gives an optimizer

$$u(t) = \sum_{k=1}^h \Re[\hat{u}_k e^{j\omega k t}], \quad \hat{u} = \operatorname{col}(\hat{u}_1, \ldots, \hat{u}_h)$$

for the original problem (12).

Proof: Let $\hat{\vartheta}_k$ and $\hat{u}_k$ be the k^{th} phasors of periodic signals $\vartheta(t)$ and $u(t)$, respectively. Using Lemma 4 in Appendix A, it can be verified that the objective function in (12) is given by

$$\frac{1}{2}\sum_{k=1}^h \begin{bmatrix}\hat{\vartheta}_k \\ \hat{u}_k\end{bmatrix}^* \Pi(j\omega k) \begin{bmatrix}\hat{\vartheta}_k \\ \hat{u}_k\end{bmatrix}$$

and the constraints are expressed as

$$\begin{aligned} &\left(2a_1 + \sum_{k=1}^h \hat{\vartheta}_k^* Q_1 \hat{\vartheta}_k\right)\nu - \sum_{k=1}^h \hat{\vartheta}_k^* S(\omega k)\hat{\vartheta}_k = 0, \\ &\hat{\vartheta}_k = P(\omega k)\hat{u}_k, \quad k \in \mathbb{Z}_h. \end{aligned}$$

The result then follows by eliminating the variable $\hat{\vartheta}_k$ through the second constraint and assembling the summations into Hermitian forms of augmented vectors. ■

For a fixed ω, the problem in (14) is a static quadratic optimization, which is nonconvex in general because $X^h(\omega)$ and $Y^h(\omega)$ are possibly indefinite. Nonconvex optimizations are

often hard to solve, but for this particular problem, we have an exact, analytical solution.

Lemma 2: Let Hermitian matrices X and Y be given and consider

$$\min_{z\in\mathbb{C}^m}\{z^*Xz : z^*Yz = 1\}. \tag{15}$$

The constraint is feasible if and only if the largest eigenvalue of Y is positive. In this case, the objective function is bounded below on the feasible set if and only if the following (convex) set is nonempty:

$$\mathbb{L} := \{\lambda \in \mathbb{R} : X \geq \lambda Y\}.$$

The largest element λ_o of $\mathbb{L}$ is well defined and is a generalized eigenvalue of (X, Y). The minimum value of (15) is equal to λ_o. An optimizer z_o is given by an eigenvector of the pair (X, Y) associated with the generalized eigenvalue λ_o, normalized so that $z_o^*Yz_o = 1$.

Proof: The minimum value in (15) is bounded below and is greater than a given value $\gamma \in \mathbb{R}$ if and only if

$$z^*Xz \geq \gamma, \quad \forall z \in \mathbb{C}^m \quad \text{s.t.} \quad z^*Yz = 1.$$

Feasibility of the constraint implies its regularity; if z_o satisfies $z_o^*Yz_o = 1$, then $z = 2z_o$ and $z_o/2$ respectively make the value of $z^*Yz - 1$ positive and negative. Hence, the S-procedure (Lemma 5 in Appendix A) can be used to verify that this condition holds if and only if there exists $\lambda \in \mathbb{R}$ such that

$$z^*Xz - \gamma \geq \lambda(z^*Yz - 1), \quad \forall z \in \mathbb{C}^m$$

which is equivalent to

$$X \geq \lambda Y, \quad \gamma \leq \lambda.$$

The minimum value in (15) is obtained by maximizing γ subject to these constraints over the variables $\lambda, \gamma \in \mathbb{R}$. Since the largest γ is equal to λ, the minimum value is given by the largest element of $\mathbb{L}$.

Let $f(\lambda)$ be the minimum eigenvalue of $X - \lambda Y$. Note that $f(\lambda)$ is a concave function of λ since the matrix is affine in λ. By feasibility of the constraint, Y must have at least one positive eigenvalue, and hence $f(\lambda)$ is negative for sufficiently large λ. On the other hand, boundedness of the objective function guarantees that $\mathbb{L}$ is nonempty, and hence $f(\lambda)$ is nonnegative for some λ. Therefore, there exists λ_o such that $f(\lambda_o) = 0$ and $f(\lambda) < 0$ for all λ greater than λ_o. Clearly, λ_o is the largest element of $\mathbb{L}$, and is a generalized eigenvalue of (X, Y).

If an eigenvector z_o of (X, Y), associated with the generalized eigenvalue λ_o, can be chosen so that $z_o^*Yz_o = 1$, then it is easy to verify that z_o is an optimizer that gives the objective function value λ_o. To show existence of such z_o, let z_ε be an eigenvector of $Z_\varepsilon := X - (\lambda_o + \varepsilon)Y$ associated with its minimum eigenvalue, where $\varepsilon \in \mathbb{R}$. Since λ_o is the largest element of $\mathbb{L}$, we have $z_\varepsilon^* Z_\varepsilon z_\varepsilon < 0$ for all $\varepsilon > 0$. Since $Z_0 \geq 0$, we have

$$0 \leq z_\varepsilon^* Z_0 z_\varepsilon = z_\varepsilon^*(Z_\varepsilon + \varepsilon Y)z_\varepsilon < \varepsilon z_\varepsilon^* Y z_\varepsilon.$$

Thus $z_\varepsilon^* Y z_\varepsilon$ is positive and therefore z_ε can be normalized so that $z_\varepsilon^* Y z_\varepsilon = 1$. In this case, $z_\varepsilon^* Z_\varepsilon z_\varepsilon < 0$ implies $z_\varepsilon^* X z_\varepsilon < \lambda_o + \varepsilon$. Now, the result follows by passing the limit $\varepsilon \downarrow 0$ and noting that $Z_\varepsilon z_\varepsilon \to 0$. ∎

Based on Lemma 2, a solution to (15) can be found by computing the generalized eigenvalues of (X, Y). If the constraint is feasible and objective function is bounded, then one (or more) of the generalized eigenvalues must be real and satisfy $X \geq \lambda Y$. The largest of such generalized eigenvalues is λ_o. If λ_o is not repeated, then it has one-dimensional eigenspace. In this case, every eigenvector z_o satisfies $z_o^* Y z_o > 0$ and hence can be normalized so that $z_o^* Y z_o = 1$. This z_o is an optimizer of (15). If λ_o is repeated, then the dimension of the eigenspace is more than one and $z_o^* Y z_o$ can be nonpositive for some eigenvector. However, Lemma 2 guarantees that there is at least one vector in the eigenspace that gives positive $z_o^* Y z_o$ and hence is a solution after the normalization.

The following result establishes that the optimal value of (14) is independent of h. The important implication is that the optimum of the original problem (12) can always be achieved by a sinusoid with a single frequency component.

Lemma 3: Consider the optimization problem (14), and denote by γ_h the optimal value of the objective function. Then, for an arbitrary $h \in \mathbb{Z}$, it holds that $\gamma_h = \gamma_1$.

Proof: In view of Lemma 2, the problem (14) can be reformulated as

$$\begin{aligned}\gamma_h &= \min_{\omega\in\mathbb{R}} \max_{\lambda\in\mathbb{R}} \left\{\lambda : X^h(\omega) \geq \lambda Y^h(\omega)\right\} \\ &= \min_{\omega\in\mathbb{R}} \max_{\lambda\in\mathbb{R}} \left\{\lambda : X(k\omega) \geq \lambda Y(k\omega), \forall k \in \mathbb{Z}_h\right\}.\end{aligned}$$

Note that, for each $k\omega$, the set of $\lambda \in \mathbb{R}$ satisfying $X(k\omega) \geq \lambda Y(k\omega)$ is convex. Using this fact, the problem can further be reformulated as

$$\begin{aligned}\gamma_h &= \min_{\omega\in\mathbb{R}} \min_{k\in\mathbb{Z}_h} \max_{\lambda\in\mathbb{R}} \{\lambda : X(k\omega) \geq \lambda Y(k\omega)\} \\ &= \min_{\omega\in\mathbb{R}} \max_{\lambda\in\mathbb{R}} \{\lambda : X(\omega) \geq \lambda Y(\omega)\} \\ &= \gamma_1.\end{aligned}$$

This completes the proof. ∎

We are now ready to state the main result.

Theorem 1: Consider the rectifier system given in (6) and the optimal locomotion problem in (12). Define $X(\omega)$, $Y(\omega)$, and $P(\omega)$ by (13). Let γ be the optimal value of the objective function. Then we have

$$\gamma = \min_{\omega\in\mathbb{R}} \max_{\lambda\in\mathbb{R}} \left\{\lambda : X(\omega) \geq \lambda Y(\omega)\right\}. \tag{16}$$

Let ω_o and λ_o be the optimizers. Then, the optimal period is $T = 2\pi/\omega_o$, and the optimal gait ϑ and input u are given by

$$u(t) = \Re[z_o e^{j\omega_o t}], \quad \vartheta(t) = \Re\left[P(\omega_o) z_o e^{j\omega_o t}\right]$$

where $z_o \in \mathbb{C}^\ell$ is the eigenvector of the pair $(X(\omega_o), Y(\omega_o))$ associated with the generalized eigenvalue λ_o, normalized to satisfy $z_o^* Y(\omega_o) z_o = 1$.

Proof: Recall that the cost function is an average value of $\xi^{\mathsf{T}}\Psi\xi$ over one cycle, where ξ is the steady state output of $F(s)$

with input $[\vartheta^{\mathsf{T}}\ u^{\mathsf{T}}]^{\mathsf{T}} \in \mathbb{P}_T$, and Ψ and $F(s)$ are defined from $\Pi(s) = F(-s)^{\mathsf{T}}\Psi F(s) \in \mathbb{\Pi}$. Since $\mathbb{P}_T$ is a subset of continuously differentiable periodic signals and $F(s)$ is a linear combination of stable transfer functions and differentiators, the signal ξ is continuous and periodic. Therefore, the signal ξ, and hence the definite integral of $\xi^{\mathsf{T}}\Psi\xi$ in the cost function, can be approximated by truncated Fourier series to an arbitrary accuracy. From Lemma 1, the problem (12) can then be characterized as the limit ($h \to \infty$) of the sequence of quadratic optimizations (14). Lemma 3 shows that the optimal value of (14) is independent of h, hence the optimal value of the original problem (12) is equal to that of (14) with $h = 1$, indicating that a sinusoid is an optimizer. The solution to the optimization over $\mathbb{P}_T^1$ is given by Lemma 2 with $h = 1$, as stated in the theorem. ■

The optimal locomotion problem (14) is nonconvex (partly) due to the velocity constraint. In general, it is difficult to find a solution to a nonconvex problem with guaranteed global optimality, since multiple local optima may exist. For our particular problem, however, it is possible to determine the global optimum with the aid of the S-procedure (Lemma 5 in Appendix A) as shown in Theorem 1. The optimal gait among all periodic functions has turned out to be a pure sinusoid for the bilinear rectifier (6). This can be viewed as a generalization of the previous result [22] that proved optimality of sinusoids when maximizing the thrust generated by a bilinear rectifier. The problem in (16) can be solved by generalized eigenvalue computation plus a line search over the frequency ω. In particular, the optimal solution, for a fixed ω, is given by the maximal real generalized eigenvalue λ_o of the pair $(X(\omega), Y(\omega))$ and the corresponding eigenvector z_o.

V. Undulatory and Flapping Gaits of the Link Chain Rectifier

In this section, we will demonstrate the utility of our optimal gait result through numerical examples. Specifically, we consider a mechanical rectifier formed by a chain of rigid links, and apply Theorem 1 to find optimal gaits with respect to several cost functions. Two nominal postures are examined; the straight posture "–" and the bow posture "(" while moving to the left. Various gaits will be shown to emerge from optimization of different cost functions with different nominal postures, including undulatory and flapping gaits as well as their hybrid.

A. Link Chain Rectifier

Consider the planar motion of a chain of n rigid links as shown in Fig. 3. For $i \in \mathbb{Z}_n$, the i^{th} link has mass m_i, moment of inertia J_i, length $2\ell_i$, and angular displacement $\theta_i(t)$ measured from the x-axis. For $i \in \mathbb{Z}_{n-1}$, the joint between the i^{th} and $(i+1)^{\text{th}}$ links is actuated by torque input u_i (when positive, the i^{th} and $(i+1)^{\text{th}}$ links tend to rotate counterclockwise and clockwise, respectively), and the joint angle is denoted by $\phi_i := \theta_i - \theta_{i+1}$. The body is placed in an environment (on the ground, in water, etc.), and is subject to the interactive forces.

The key property for mechanical rectification is the difference in the tangential and normal components of the interactive force from the environment acting on each link. In particular, the normal force tends to be much larger than the tangential force (e.g., snake crawling on the ground [24] and slender-body swimming [28]–[30]). The simplest way to capture this property, which is often adequate for at least qualitative analyses, is to approximate the tangential and normal forces on each link (f_{t_i} and f_{n_i}) by linear functions of the respective components of the relative velocity between the link and environment (v_{t_i} and v_{n_i}). That is, for the i^{th} link

$$f_{t_i} = c_{t_i} v_{t_i}, \quad f_{n_i} = c_{n_i} v_{n_i} \tag{17}$$

where c_{t_i} and c_{n_i} are constants such that $c_{t_i} \ll c_{n_i}$. The linear model in (17) may be obtained from direct curve fitting of experimental data, or from (quasi)linearization of a more realistic nonlinear model. We call the system under this type of directional forces a link chain rectifier (LCR).

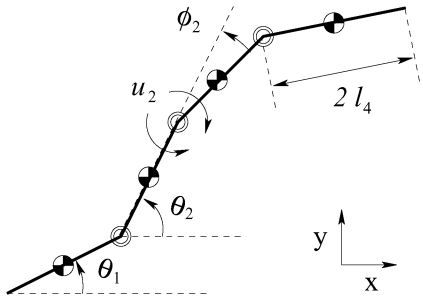

Fig. 3. Link chain rectifier.

The general equations of motion for the LCR have been derived in an attempt to model robotic snake locomotion [8], and are of the form given by (3). Motion dynamics near an arbitrary nominal posture η can be approximated by the bilinear rectifier (6). The details of the models are summarized in Appendix B. The models thus developed naturally capture the dynamics of slender animals that undulate for locomotion, such as crawling snake [8], [24], and swimming leech and lamprey [31]–[33]. While the nominal posture for such undulatory locomotion would be straight, optimizations at another nominal posture will lead to flapping gaits, as shown later.

For the planar case ($p = 2$), the term $L(\vartheta)$ for rectifying dynamics in (6) has the form $[\Lambda_1\vartheta\ \Lambda_2\vartheta]$. The model for LCR defined in Appendix B shows that, regardless of the nominal posture η, the skew-symmetric part of Λ_k is zero (in fact Λ_k is diagonal) for $k \in \mathbb{Z}_2$ if the environmental interactive force has no directional preference, i.e., $c_{t_i} = c_{n_i}$ for $i \in \mathbb{Z}_n$. In this case, the net thrust over a cycle is zero for any periodic body motion as seen in (7). This is a proof that the directional preference in the environmental force is essential for locomotion of LCR.

For the numerical studies reported below, we set the parameter values from measured data of a medium size leech to keep the model realistic. The leech has mass $m = 1.1$ g and length $\ell = 107.3\,\text{mm}$, and was observed to swim at speed around 0.157 m/s by undulating its slender body like snakes with a cycle frequency near 2.7 Hz. The leech has a segmented body that can be modeled by a chain of n identical links where $n = 18$.

B. Undulatory Gait

We set the nominal posture to be straight ($\eta = 0$). No stiffness or damping is assumed at the body joints. The parameters of the bilinear rectifier (6) for this case are summarized at the end of

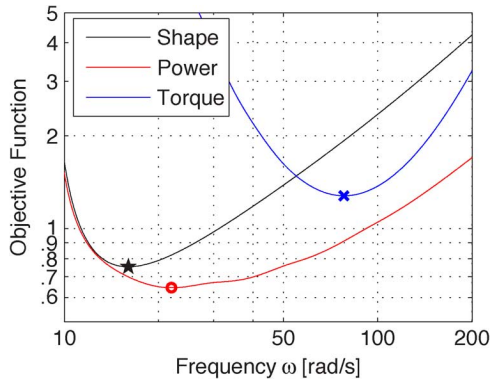

Fig. 4. Objective function versus frequency ω: power in mW, torque in $(\mathrm{N}\cdot\mathrm{mm}*100)^2$, shape derivative in $(\mathrm{deg/ms})^2$.

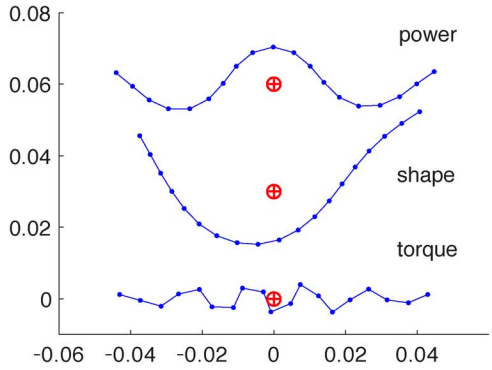

Fig. 5. Optimal body shapes (snap shots during swimming at an arbitrary time instant).

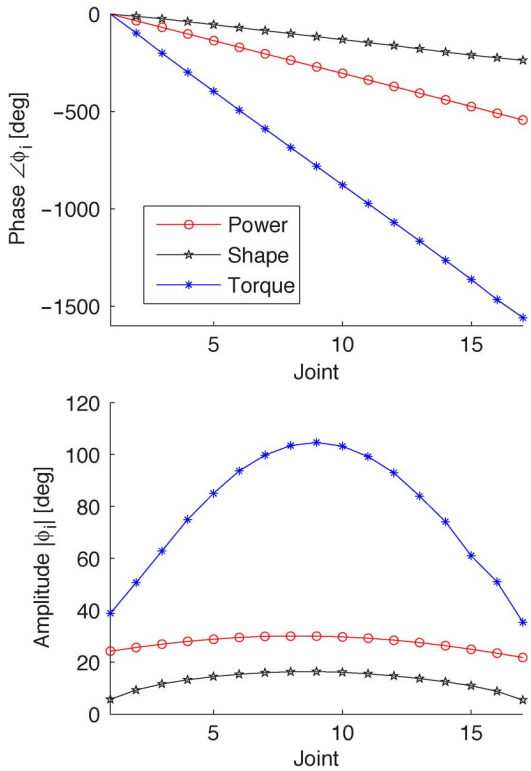

Fig. 6. Undulatory gaits: phase and amplitude of relative angles ϕ_i along the body.

Appendix B. Assuming an average velocity of $\nu = -0.157\ \mathrm{m/s}$ (negative sign indicates swimming to the left), the optimal gait problem (12) is solved for three cost functions in Table I: input power, input torque, and shape derivative where $W := B$. The optimal gait for each case has been found by solving (16) via eigenvalue computations with frequency sweep.

Fig. 4 shows the minimum value of each objective function as a function of frequency ω, which is the maximum real generalized eigenvalue of the pair $(X(\omega), Y(\omega))$ in (13). Each function turned out to be quasi-convex and have a unique global minimum for this particular example. The optimal cycle frequencies of periodic body motion are found to be 22.0 rad/s (power), 78.1 rad/s (torque), and 16.0 rad/s (shape), whereas the frequency observed for the particular leech used for modeling was 17.0 rad/s. The optimal body shapes are shown in Fig. 5. These shapes are generated from the phases and amplitudes (Fig. 6) of the shape variables (joint angles) ϕ_i. In each figure, the leech head/tail is to the left/right. The phase angle decreases from head to tail, indicating waves traveling down the body to generate thrust. The number of waves expressed by the body is roughly equal to the phase lag from head to tail, divided by 360°. During swimming, the live leech exhibited about 250° phase lag, and approximately uniform (but slightly increasing toward the tail) amplitudes over the body of about 10°. The resulting body shape was fairly close to the one for the minimum shape derivative depicted in Fig. 5. Hence, it is tempting to conclude that the shape derivative, rather than the power or torque, may be closely related to the quantity that actual leeches try to minimize.

C. Flapping Gait

In the previous section, the nominal posture was chosen to be straight with the locomotion velocity vector v_o aligned with the body. We now consider the situation where the body is initially straight and is *perpendicular* to v_o. The body would then be bent due to the fluid drag, and, with flexible joints, take a bow posture "(" when it moves to the left and the drag balances with the restoring stiffness force. We choose this as the nominal posture. In particular, η is set so that η_i linearly decreases from $\eta_1 = \pi - 0.068$ to $\eta_n = 0.068$ rad. Assuming an average velocity of $\nu = -0.1\ \mathrm{m/s}$ (negative sign indicates swimming to the left), the joint stiffnesses k_i $(i \in \mathbb{Z}_{n-1})$ have been specified so that the first condition in (5) is satisfied. Gaits expected at this nominal posture include two flagella pushing a central body forward, or a radially symmetric jellyfish-like locomotion.

We have solved the optimal locomotion problem in (12) with objective function Π in (10) where Π_a captures the perturbation from η, and Π_o captures the shape derivative, input torque rate, or input power as indicated in Table I. For each case, the optimal gait was computed using Theorem 1, where the scalar weight β was tuned by iteration so that the amplitude constraint $\|\hat{\vartheta}\|^2 = 10$ was satisfied, as described in Section IV-A. The results of the three optimizations are summarized in terms of $\varphi := B^{\mathsf{T}}\vartheta$, which are the joint angle deflections from the nominal posture. Numerical simulations are then used to examine the effects of approximations associated with the equations of motion and the optimal gait problem. Unless otherwise noted,

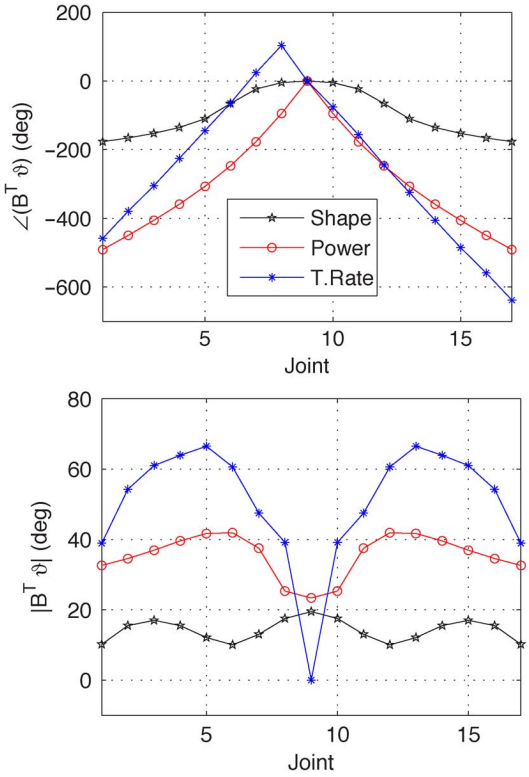

Fig. 7. Flapping gaits: phase and amplitude of relative angle perturbations $B^{\mathsf{T}}\vartheta$ along the body.

TABLE II
OPTIMAL FREQUENCIES [rad/s] AND SIMULATED VELOCITIES [mm/s]

Quantity	Optimal ω	Nonlinear v	Bilinear v
Power	39.7	-69.8	-100.7
Shape Derivative	30.5	-82.8	-107.9
Torque Rate	83.9	-67.4	-100.3

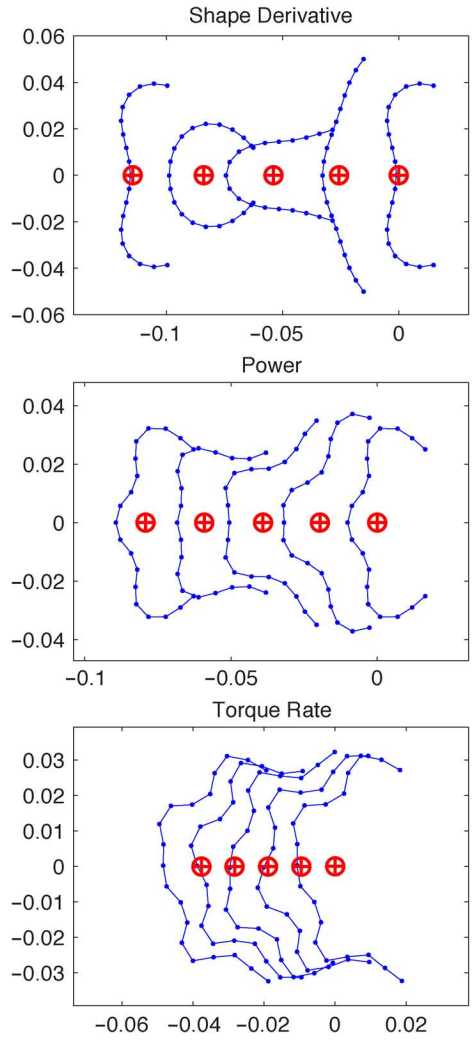

Fig. 8. Snap shots of LCR locomotion, taken 1.25 periods apart.

the second equation in (6) is simulated by enforcing the calculated optimal gait $\theta(t)$ as the input.

Fig. 7 shows the phase and amplitude of φ for the three optimal gaits whose frequencies are summarized in Table II. We see that the phase is maximum at or around the middle of the body and decreases toward both ends. This means that all three gaits possess some degree of traveling waves down each arm. However, the minimum shape derivative motion has a much smaller phase variation than the power or torque rate case, indicating that it has a much lower number of waves expressed along the body. It should be noted that the torque rate criterion generated an asymmetric gait. After checking this result against the optimal gait under the symmetry constraint, we found that the asymmetric gait did indeed have a strictly smaller minimum objective value. Among the three cases, the average amplitude over the body tends to be smaller if the phase variation is smaller. This is because small, relatively in-phase, joint angle amplitudes add up to produce a large overall motion which maintains the desired velocity. Interestingly, the torque rate case does not bend at all at the center joint (only rotates), retaining its initial nominal bend at all times.

Fig. 8 shows five snapshots of simulated optimal locomotion for each case, taken 1.25 periods apart. These figures clearly show that the optimal motion calculated for minimum power and shape derivative are symmetric about the direction of locomotion (horizontal axis). The asymmetry is clearly visible for the torque rate case. The flapping gait is found optimal for the shape derivative criterion, while undulation of each arm is optimal for the torque rate criterion. The optimal gait for the power criterion is a mixture of flapping and undulation. The horizontal axis scales are different in each figure due to the differing optimal frequencies calculated for each motion; for example the shape derivative motion moves much further in five periods than the torque rate motion, although the locomotion speeds are about the same.

Fig. 9 shows the simulated velocity, where the time responses are colored in the same way as Fig. 7 for each case. We see that the y-velocity is exactly zero for the symmetric gaits, and oscillating closely about zero for the asymmetric gait. Thus, as expected, the optimization forces the y-velocity to be zero on average even though no such constraint is explicitly imposed. The oscillation of the x-velocity is small in the power and torque rate cases, but is much larger in the shape derivative case due to the large stroking motion of the arms. The non-sinusoidal shape

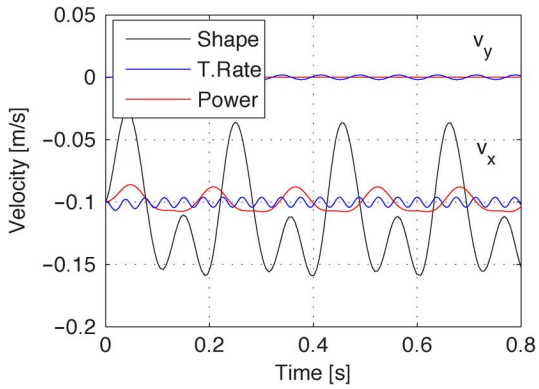

Fig. 9. Simulated CG velocity.

in the shape derivative case results from higher frequency components which can be explained by thinking of a flipping fish tail: for one period of motion the tail produces two thrusts. The varying magnitude of the x-velocity results from the alternating high and low drag associated with the arms being extended out or folded back during the stroke. In general, the higher the wave number and frequency a motion possesses, the smaller the perturbation about the desired average velocity.

Finally, average x-velocities are summarized in Table II. The "nonlinear ν" and "bilinear ν" indicate the average velocities calculated from simulations of the second equation in (3) and (6), respectively. For the bilinear rectifier, the simulated average velocities are close to $\nu = -0.1\ \mathrm{m/s}$ at which the optimal gaits are calculated, despite the fact that oscillations of ν around this value are ignored during the optimization. On the other hand, the higher order nonlinearity tends to reduce the actual swim speed. The gaits found from the bilinear rectifier equations may be away from optimality for the original fully nonlinear equations of motion. Nevertheless, the basic gaits thus found do lead to reasonable locomotion of the original system, and may be used as the initial condition for further optimizations that would necessarily be local due to the system complexity.

VI. Conclusion

We have defined a general class of mechanical rectifier systems that captures the essential dynamics of animal locomotion. An optimal gait problem was formulated to minimize a quadratic cost function while achieving a given speed of locomotion on average. The solution was shown to be purely sinusoidal, and calculated from generalized eigenvalues and eigenvectors of a pair of Hermitian matrices as frequency was varied. This is a very fast and numerically stable method capable of handling underactuated and hyper-redundant systems while ensuring achievability. Unlike most, if not all, of existing approaches, our result provides a globally optimal solution. The key is not to compromise the solution by aiming for local optimality, but to reformulate the problem for tractability, in terms of a simplified model capturing the essential rectifier dynamics. The optimal gait thus obtained can be used as a reference signal for closed-loop control. Moreover, it can also be used, if desired, as an initial condition for the existing local algorithms to refine the gait for a more complex, fully nonlinear model of the rectifier dynamics.

The case studies have shown that the quadratic optimization can produce gaits that closely resemble those seen in biology. In particular, for the link chain rectifier with a straight nominal posture, the gait minimizing the shape derivative was found similar to the natural motion exhibited in swimming leeches. For the link chain rectifier with a curved nominal posture, most optimal gaits were found to be symmetric, agreeing with our intuition based on biological observations of swimming jellyfish-like animals. The gait which minimized the torque derivative was found to be asymmetric, however, indicating that some systems may benefit from unconventional gaits that are not commonly observed in biology and counter to intuition.

Finally, these studies demonstrate that the proposed framework for computing optimal gaits can be very useful, not only for robotic locomotor designs, but also for increasing our understanding of animal locomotion mechanisms from a biological point of view. The models of rectifier systems could be used as a basis for further analysis and design of locomotion control systems. Of particular interest is the limit cycle behaviors of the rectifier systems driven by biological feedback control systems called central pattern generators [34]–[38].

Appendix A
Preliminary Lemmas

Lemma 4: Let $h \in \mathbb{Z}_\infty$, a positive number $T \in \mathbb{R}$, a vector-valued signal $\mu \in \mathbb{P}_T^h$ and a transfer function $\Pi(s) = F(-s)^{\mathsf{T}} \Phi F(s) \in \mathbb{\Pi}$ be given. Let ξ be the steady state response of $F(s)$ with input μ. Then the following hold:

$$\hat{\xi} = F^h(j\omega)\hat{\mu}, \quad \hat{\xi}_k = F(j\omega k)\hat{\mu}_k, \quad \forall k \in \mathbb{Z},$$

$$\frac{2}{T}\int_0^T \mu^{\mathsf{T}} \overset{\circ}{\Pi}\, \mu dt = \sum_{k=1}^{h} [\hat{\mu}_k^* \Pi(j\omega k)\hat{\mu}_k] = \hat{\mu}^* \Pi^h(j\omega)\hat{\mu}$$

where $\omega := 2\pi/T$.

Proof: The result follows from straightforward calculation using basic properties of linear systems and orthogonality of harmonic basis functions. ∎

Lemma 5 (S-Procedure [39]): Let real-valued quadratic functionals σ_o and σ_1 on a complex linear space $\mathbb{X}$ be given, where each has the form $\sigma(x) = a + \Re[b(x)] + C(x)$ with a real constant a, linear functional $b(x)$ on $\mathbb{X}$, and Hermitian form $C(x)$. Suppose σ_1 satisfies the regularity condition: there exist $y, z \in \mathbb{X}$ such that $\sigma_1(y) > 0$ and $\sigma_1(z) < 0$. Then

$$\sigma_o(x) \geq 0, \quad \forall x \in \mathbb{X} \quad \text{such that} \quad \sigma_1(x) = 0$$

holds if and only if

$$\exists \lambda \in \mathbb{R} \quad \text{such that} \quad \sigma_o(x) \geq \lambda \sigma_1(x), \quad \forall x \in \mathbb{X}.$$

APPENDIX B
LINK CHAIN RECTIFIER MODEL

The link chain rectifier has been introduced as a model for robotic snakes [8], and the equations of motion are given by (3) with the following definitions:

$$
\begin{aligned}
C(\theta,\dot\theta)\dot\theta &:= (S_\theta H C_\theta - C_\theta H S_\theta)\dot\theta^2,\\
J_o &:= \mathrm{diag}(J_1,\dots,J_n),\\
J(\theta) &:= J_o + S_\theta H S_\theta + C_\theta H C_\theta,\\
M &:= \mathrm{diag}(m_1,\dots,m_n),\\
F &:= M^{-1}B(B^{\mathsf T}M^{-1}B)^{-1}A^{\mathsf T}L,\\
C_n &:= \mathrm{diag}\,(c_{n_1},\dots,c_{n_n}),\\
C_\theta &:= \mathrm{diag}(\cos\theta_1,\dots,\cos\theta_n),\\
K_o &:= \mathrm{diag}(k_1,\dots,k_{n-1}),\\
S_\theta &:= \mathrm{diag}(\sin\theta_1,\dots,\sin\theta_n),\\
D_o &:= \mathrm{diag}(d_1,\dots,d_{n-1}),\\
H &:= LA(B^{\mathsf T}M^{-1}B)^{-1}A^{\mathsf T}L,\\
\Gamma &:= \mathrm{diag}(C_t, C_n, C_nL^2/3),\\
C_t &:= \mathrm{diag}\,(c_{t_1},\dots,c_{t_n}),\\
d(\theta,\dot\theta) &= BD_oB^{\mathsf T}\dot\theta, \quad B(\theta) := B,\\
k(\theta) &= BK_oB^{\mathsf T}\theta, \quad L := \mathrm{diag}(\ell_1,\dots,\ell_n),\\
m &:= \sum_{i=1}^{n} m_i, \quad \gamma(x) := \Gamma x,\\
\Omega_\theta &:= \begin{bmatrix} C_\theta & S_\theta \\ -S_\theta & C_\theta \end{bmatrix}, \quad G_\theta := \begin{bmatrix} FS_\theta \\ -FC_\theta \end{bmatrix},\\
e &:= \begin{bmatrix} 1 \\ \vdots \\ 1 \end{bmatrix}, \quad R(\theta) := \begin{bmatrix} \Omega_\theta G_\theta \\ I \end{bmatrix},\\
N(\theta) &:= \begin{bmatrix} \Omega_\theta E \\ 0 \end{bmatrix}, \quad E := \begin{bmatrix} e & 0 \\ 0 & e \end{bmatrix},\\
A &:= \begin{bmatrix} 1 & 1 & & \\ & \ddots & \ddots & \\ & & 1 & 1 \end{bmatrix}^{\mathsf T},\\
B &:= \begin{bmatrix} 1 & -1 & & \\ & \ddots & \ddots & \\ & & 1 & -1 \end{bmatrix}^{\mathsf T}
\end{aligned}
$$

where $A, B \in \mathbb{R}^{n\times(n-1)}$, $e \in \mathbb{R}^n$, and $\dot\theta^2$ is the vector whose i^{th} entry is $\dot\theta_i^2$. Given a nominal posture η, the bilinear rectifier model that approximates the original system is given by (6) with

$$
\begin{aligned}
Q(\vartheta) &:= N_\eta^{\mathsf T}\Gamma N_\eta + \Xi\Theta + (\Xi\Theta)^{\mathsf T} + \Theta^{\mathsf T}\Psi\Theta,\\
K &:= BK_oB^{\mathsf T}, \quad A(\vartheta) := R_\eta^{\mathsf T}\Gamma N_\eta + [\Lambda_1\vartheta \;\; \Lambda_2\vartheta],\\
[\lambda_1 \;\; \lambda_2] &:= \dot R_1^{\mathsf T}\Gamma N_\eta, \quad D := BD_oB^{\mathsf T} + R_\eta^{\mathsf T}\Gamma R_\eta,\\
\Psi &:= \dot{\mathcal{U}}_\eta^{\mathsf T}\Gamma\dot{\mathcal{U}}_\eta + \Delta + \Delta^{\mathsf T},\\
J &:= J(\eta), \quad \Xi := N_\eta^{\mathsf T}\Gamma\dot{\mathcal{U}}_\eta, \quad \Theta := \mathrm{diag}(\vartheta,\vartheta),\\
[\Lambda_1 \;\; \Lambda_2] &:= [\mathrm{diag}(\lambda_1) \;\; \mathrm{diag}(\lambda_2)] + R_\eta^{\mathsf T}\Gamma\dot{\mathcal{U}}_\eta + \dot R_2^{\mathsf T}\Gamma\mathcal{U}_\eta,\\
\Delta &:= \begin{bmatrix} \mathrm{diag}(\delta_1) & \mathrm{diag}(\delta_2) \\ \mathrm{diag}(\delta_3) & \mathrm{diag}(\delta_4) \end{bmatrix},\\
\begin{bmatrix} \delta_1 & \delta_2 \\ \delta_3 & \delta_4 \end{bmatrix} &:= -N_\eta^{\mathsf T}\Gamma\mathcal{U}_\eta/2, \quad \dot R_1 := \begin{bmatrix} \Omega_\eta\dot G_\eta \\ 0 \end{bmatrix},\\
\dot R_2 &:= \begin{bmatrix} \dot\Omega_\eta \\ G_\eta \\ 0 \end{bmatrix}, \quad \dot G_\eta := \begin{bmatrix} FC_\eta \\ FS_\eta \end{bmatrix},\\
\dot\Omega_\eta &:= \begin{bmatrix} -S_\eta & C_\eta \\ -C_\eta & -S_\eta \end{bmatrix}, \quad \mathcal{U}_\eta := \begin{bmatrix} \Omega_\eta \\ 0 \end{bmatrix}, \quad \dot{\mathcal{U}}_\eta := \begin{bmatrix} \dot\Omega_\eta \\ 0 \end{bmatrix}
\end{aligned}
$$

where the subscript η is used to indicate that a function is evaluated at $\theta = \eta$, e.g. $N_\eta := N(\eta)$. If the nominal posture is chosen to be straight ($\eta = 0$), then these parameter definitions simplify to

$$
\begin{aligned}
J &:= J_o + F^{\mathsf T}MF,\\
D &:= LC_nL/3 + F^{\mathsf T}C_nF + BD_oB^{\mathsf T},\\
\Lambda &:= F^{\mathsf T}C_o + \mathrm{diag}(F^{\mathsf T}C_te),\\
A(\vartheta) &:= [\Lambda\vartheta \quad -F^{\mathsf T}C_ne],\\
Q(\vartheta) &:= \begin{bmatrix} e^{\mathsf T}C_te + \vartheta^{\mathsf T}C_o\vartheta & -\vartheta^{\mathsf T}C_oe \\ -e^{\mathsf T}C_o\vartheta & e^{\mathsf T}C_ne - \vartheta^{\mathsf T}C_o\vartheta \end{bmatrix},\\
C_o &:= C_n - C_t.
\end{aligned}
$$

Additionally, if $c_{n_i} := c_n$ and $c_{t_i} := c_t$ for all i, the equations are further reduced by noting that $F^{\mathsf T}e = 0$. The following parameter values are from a typical medicinal leech, and are used for the model in the numerical study reported here unless otherwise noted:

$$
\begin{aligned}
&n = 18, \quad m = 0.0011\,\mathrm{kg}, \quad \ell = 0.1073\,\mathrm{m}, \quad m_i = m/n,\\
&c_{n_i} = 0.8\ell_i\,\mathrm{N\cdot s/m}, \quad c_{t_i} = 0.1\ell_i\,\mathrm{N\cdot s/m},\\
&\ell_i = \ell/(2n), \quad J_i := m_i\ell_i^2/3, \quad d_i = 0, \quad k_i = 0.
\end{aligned}
$$

ACKNOWLEDGMENT

The authors thank Dr. W.O. Friesen and J. Chen, University of Virginia, for providing the measured data for a leech.

REFERENCES

[1] B. D. O. Anderson, *Personal Communication.* 1998.

[2] R. W. Brockett, "On the rectification of vibratory motion," *Sensors Actuators*, vol. 20, pp. 91–96, 1989.

[3] D. F. Hoyt and C. R. Taylor, "Gait and the energetics of locomotion in horses," *Nature*, vol. 292, pp. 239–240, 1981.

[4] F. J. Diedrich and W. H. Warren, "Why change gaits—Dynamics of the walk run transition," *J. Exper. Psychol.—Human Perception Perform.*, vol. 21, no. 1, pp. 183–202, 2000.

[5] M. Sfakiotakis, D. M. Lane, and J. B. C. Davies, "Review of fish swimming modes for aquatic locomotion," *IEEE J. Oceanic Eng.*, vol. 24, no. 2, pp. 237–252, Apr. 1999.

[6] A. J. Ijspeert, A. Crepsi, D. Ryczko, and J. M. Cabelguen, "From swimming to walking with a salamander robot driven by a spinal cord model," *Science*, vol. 315, no. 5817, pp. 1416–1420, 2007.

[7] C. Chevallereau and Y. Aoustin, "Optimal reference trajectories for walking and running of a biped robot," *Robotica*, vol. 19, pp. 557–569, 2001.

[8] M. Saito, M. Fukaya, and T. Iwasaki, "Serpentine locomotion with robotic snake," *IEEE Control Syst. Mag.*, vol. 22, no. 1, pp. 64–81, 2002.

[9] K. A. McIsaac and J. P. Ostrowski, "Motion planning for anguilliform locomotion," *IEEE Trans. Robot. Autom.*, vol. 19, no. 4, pp. 637–652, Apr. 2003.

[10] J. Cortes, S. Martinez, J. P. Ostrowski, and K. A. McIsaac, "Optimal gaits for dynamic robotic locomotion," *Int. J. Robot. Res.*, vol. 20, no. 9, pp. 707–728, 2001.

[11] T. Saidouni and G. Bessonnet, "Generating globally optimised sagittal gait cycles of a biped robot," *Robotica*, vol. 21, no. 2, pp. 199–210, 2003.
[12] M. Srinivasan and A. Ruina, "Computer optimization of a minimal biped model discovers walking and running," *Nature*, vol. 439, no. 7072, pp. 73–75, 2006.
[13] J. P. Ostrowski, J. P. Desai, and V. Kumar, "Optimal gait selection for nonholonomic locomotion systems," *Int. J. Robot. Res.*, vol. 19, pp. 225–237, 2000.
[14] G. Bessonnet, S. Chesse, and P. Sardain, "Optimal gait synthesis of a seven-link planar biped," *Int. J. Robot. Res.*, vol. 23, no. 10–11, pp. 1059–1073, 2004.
[15] G. Hicks and K. Ito, "A method for determination of optimal gaits with application to a snake-like serial-link structure," *IEEE Trans. Autom. Control*, vol. 50, no. 9, pp. 1291–1306, Sep. 2005.
[16] J. Blair and T. Iwasaki, "On the optimal harmonic gait for locomotion of mechanical rectifier systems," in *Proc. IFAC World Congress*, 2008, pp. 1723–1728.
[17] J. Blair and T. Iwasaki, "A further result on the optimal harmonic gait for locomotion of mechanical rectifier systems," in *Proc. Amer. Control Conf.*, 2009, pp. 1742–1747.
[18] M. W. Spong and M. Vidyasagar, *Robot Dynamics and Control*. New York: Wiley, 1989.
[19] R. E. Skelton and M. C. de Oliveira, *Tensegrity Systems*. New York: Springer, 2009.
[20] T. Bliss, T. Iwasaki, and H. Bart-Smith, "CPG control of a tensegrity morphing structure for biomimetic applications," *Adv. Sci. Technol.*, vol. 58, pp. 137–142, 2008.
[21] T. Iwasaki, "Coordinated rhythmic motion by uncoupled neuronal oscillators with sensory feedback," *J. Control, Meas., Syst. Integr.*, vol. 1, no. 2, pp. 165–174, 2008.
[22] Z. Chen and T. Iwasaki, "Circulant synthesis of central pattern generators with application to control of rectifier systems," *IEEE Trans. Autom. Control*, vol. 53, no. 2, pp. 273–286, Mar. 2008.
[23] H. K. Khalil, *Nonlinear Systems*. Englewood Cliffs, NJ: Prentice Hall, 1996.
[24] S. Hirose, *Biologically Inspired Robots: Snake-Like Locomotors and Manipulators*. Oxford, U.K.: Oxford Univ. Press, 1993.
[25] D. L. Hu, J. Nirody, T. Scott, and M. J. Shelley, "The mechanics of slithering locomotion," *Proc. Nat. Acad. Sci.*, vol. 106, no. 25, pp. 10081–10085, 2009.
[26] R. W. Brockett, "Pattern generation and the control of nonlinear systems," *IEEE Trans. Autom. Control*, vol. 48, no. 10, pp. 1699–1711, Oct. 2003.
[27] G. Zhu and R. E. Skelton, "Mixed L_2 and L_∞ problems by weight selection in quadratic optimal control," *Int. J. Control*, vol. 53, no. 5, pp. 1161–1176, 1991.
[28] G. Taylor, "Analysis of the swimming of long and narrow animals," *Proc. Royal Soc. London. Series A*, vol. 214, no. 1117, pp. 158–183, 1952.
[29] M. J. Lighthill, "Note on the swimming of slender fish," *J. Fluid Mech.*, vol. 9, pp. 305–317, 1960.
[30] T. McMillen and P. Holmes, "An elastic rod model for anguilliform swimming," *J. Math. Biol.*, vol. 53, no. 5, pp. 843–886, 2006.
[31] G. Bowtell and T. L. Williams, "Anguilliform body dynamics: Modeling the interaction between muscle activation and body curvature," *Phil. Trans. R. Soc. Lond. B*, vol. 334, pp. 385–390, 1991.
[32] O. Ekeberg, "A combined neuronal and mechanical model of fish swimming," *Biol. Cybern.*, vol. 69, no. 5/6, pp. 363–374, 1993.
[33] C. E. Jordan, "Coupling internal and external mechanics to predict swimming behavior: A general approach?," *Amer. Zool.*, vol. 37, pp. 710–722, 1996.
[34] T. Iwasaki and M. Zheng, "Sensory feedback mechanism underlying entrainment of central pattern generator to mechanical resonance," *Biol. Cybern.*, vol. 94, no. 4, pp. 245–261, 2006.
[35] T. Iwasaki, "Multivariable harmonic balance for central pattern generators," *Automatica*, vol. 44, no. 12, pp. 4061–4069, 2008.
[36] Y. Futakata and T. Iwasaki, "Formal analysis of resonance entrainment by central pattern generator," *J. Math. Biol.*, vol. 57, no. 2, pp. 183–207, 2008.
[37] Z. Chen, M. Zheng, W. O. Friesen, and T. Iwasaki, "Multivariable harmonic balance analysis of neuronal oscillator for leech swimming," *J. Comput. Neurosci.*, vol. 25, no. 3, pp. 583–606, 2008.
[38] Z. Chen and T. Iwasaki, "Matrix perturbation analysis for weakly coupled oscillators," *Syst. Control Lett.*, vol. 58, no. 2, pp. 148–154, 2009.
[39] A. L. Fradkov and V. A. Jakubovic, "The S-procedure and a duality relations in nonconvex problems of quadratic programming," *Vestnik Leningrad Univ. Math.*, vol. 6, no. 2, pp. 101–109, 1979, (English translation of a Russian publication in 1973).

Justin Blair was born in Winchester, VA, in 1980. He received the B.S. degree (with distinction) from the Mechanical and Aerospace Engineering (MAE) Department, School of Engineering and Applied Science, University of Virginia (UVA), Charlottesville, VA, in 2002 and is currently pursuing the Ph.D. degree in mechanical engineering (with a concentration in dynamics and control) at the Department of Mechanical and Aerospace Engineering (MAE), the University of Virginia (UVA), Charlottesville.

He was employed from 2002 to 2003 as a Mechanical Engineer at the Naval Surface Warfare Center, Dahlgren, VA. Presently, he is a Research Assistant in the Multidisciplinary University Research Initiative (MURI) Team, UVA's MAE Department. His research interests include the dynamics and control of animal locomotion through modeling and analysis.

Mr. Blair is a member of the American Society of Mechanical Engineers (ASME) and is a certified member of the honorary Mechanical Engineering fraternity, Pi Tau Sigma.

Tetsuya Iwasaki (F'09) received the B.S. and M.S. degrees in electrical and electronic engineering from the Tokyo Institute of Technology (Tokyo Tech), Tokyo, Japan, in 1987 and 1990, respectively, and the Ph.D. degree in aeronautics and astronautics from Purdue University, West Lafayette, IN, in 1993.

He joined the UCLA faculty in 2009 as Professor of Mechanical and Aerospace Engineering. He held a Post-Doctoral Research Associate position at Purdue University (1994–1995), and faculty positions at Tokyo Tech (1995–2000) and at the University of Virginia, Charlottesville (2000–2009). He was an Associate Editor for *Systems & Control Letters*, *IFAC Automatica*, and the *International Journal of Robust and Nonlinear Control*. His current research interests include biological control mechanisms underlying animal locomotion, nonlinear oscillators, and robust/optimal control theories and their applications to mechanical, aerospace, and electrical systems.

Dr. Iwasaki received the CAREER Award from the National Science Foundation (NSF), the Pioneer Prize from SICE, the George S. Axelby Outstanding Paper Award from The IEEE, and the Rudolf Kalman Best Paper Award from the ASME. He has served as Associate Editor of the IEEE TRANSACTIONS ON AUTOMATIC CONTROL. He is a member of ASME.